

# Quantitative phase imaging with programmable illumination

Taewoo Kim<sup>a</sup>, Chris Edwards<sup>b</sup>, Lynford L. Goddard<sup>b</sup>, Gabriel Popescu<sup>a\*</sup>

<sup>a</sup> Quantitative Light Imaging Laboratory, Department of Electrical and Computer Engineering, Beckman Institute for Advanced Science and Technology, University of Illinois at Urbana-Champaign, Urbana, Illinois 61801, USA; <sup>b</sup> Photonic Systems Laboratory, Department of Electrical and Computer Engineering, Micro and Nanotechnology Laboratory, University of Illinois at Urbana-Champaign, Urbana, Illinois 61801, USA

## ABSTRACT

Even with the recent rapid advances in the field of microscopy, non-laser light sources used for light microscopy have not been developing significantly. Most current optical microscopy systems use halogen bulbs as their light sources to provide a white-light illumination. Due to the confined shapes and finite filament size of the bulbs, little room is available for modification in the light source, which prevents further advances in microscopy.

By contrast, commercial projectors provide a high power output that is comparable to the halogen lamps while allowing for great flexibility in patterning the illumination. In addition to their high brightness, the illumination can be patterned to have arbitrary spatial and spectral distributions. Therefore, commercial projectors can be adopted as a flexible light source to an optical microscope by careful alignment to the existing optical path.

In this study, we employed a commercial projector source to a quantitative phase imaging system called spatial light interference microscopy (SLIM), which is an outside module for an existing phase contrast (PC) microscope. By replacing the ring illumination of PC with a ring-shaped pattern projected onto the condenser plane, we were able to recover the same result as the original SLIM. Furthermore, the ring illumination is replaced with multiple dots aligned along the same ring to minimize the overlap between the scattered and unscattered fields. This new method minimizes the halo artifact of the imaging system, which allows for a halo-free high-resolution quantitative phase microscopy system.

**Keywords:** Quantitative phase imaging, Microscopy, Interference, Phase shifting, Patterned illumination, Optogenetics, SLIM

## 1. INTRODUCTION

Quantitative phase imaging (QPI) is a rapidly emerging field used not only to visualize biological cells and tissues that are essentially transparent under the visible spectrum [1, 2], but also to obtain biological information such as cell dry mass [3-5], membrane dynamics [6-19], intracellular or intercellular transport [5, 20, 21], and 3D cellular structures [22-31]. Moreover, this variety of information can also be used for diagnostic tools to perform a number of clinical applications such as blood screening and cancer diagnosis [3, 32-39]. Outside of biology, QPI has found exciting applications in materials science where it has been used to optically monitor wet etching, photochemical etching, dissolution of biodegradable electronics, and even the expansion and deformation of materials for sensing applications [40-44]. Spatial light interference microscopy (SLIM) is a QPI method based on the phase shifting method to obtain quantitative phase of a transparent sample [45]. SLIM obtains four interferograms, or phase contrast images, that are generated from the interference between the reference and the scattered optical field with a phase shift of  $0$ ,  $\pi/2$ ,  $\pi$ , or  $3\pi/2$ . This phase shifting is done in the Fourier plane formed by a Fourier lens located at a focal distance away from the image plane of the microscope because at this point the reference and scattered fields are spatially separated. Combining these four frames, the phase shift from the object can be quantitatively and uniquely determined with a 0.28 nm spatial sensitivity and a 0.029 nm temporal sensitivity is obtained [45]. One drawback of SLIM is the limitation coming from the commercial microscope because they have components that are designed specifically for the microscope. For example, it does not utilize the full numerical aperture (NA) of the condenser, because the illumination annulus is much smaller than the condenser. This prevents the maximum possible resolution since the resolution of an optical imaging system is proportional to the sum of the condenser NA and the objective NA. In order to solve some of the limitations and to obtain a more accurate quantitative phase imaging method, we introduce a programmable illumination to the SLIM system, and as a first step, we present an upgraded SLIM with a programmable illumination source.

## 2. SLIM WITH A PROGRAMMABLE ILLUMINATION

SLIM with a programmable illumination includes three parts: programmable illumination, phase contrast microscope and SLIM module. The schematic of the system is shown in Fig. 1a. The illumination consists of a projector (EPSON Home Cinema 5030UB), an imaging lens (L1) and a lens system (FLS) that forms a Fourier transform at the original location of the microscope halogen bulb ( $P_b$ ). The lens in dashed line in FLS can be removed to project the image from the projector to  $P_b$ , instead of projecting the Fourier transform of the image. Therefore, the effective focal length of FLS is a half of the distance from  $IP_p$  to  $P_b$ . The Fourier transform of the projected pattern has to form at  $P_b$  in order to match with the alignment inside the microscope, which basically takes the bulb as a point source. Through proper alignment, a point source equivalent with structural information can be generated at the illumination plane, which is then collected by the collector lens of the microscope. The diffuser, white-light filter and the annulus of the microscope are removed in the setup to preserve the spatial and spectral pattern recorded in the illumination. The illumination is then focused at the sample plane, and scatters through the sample. The scattered field at the sample plane is collected by the objective lens and imaged at the image plane ( $IP_M$ ) through the tube lens of the microscope, entering the SLIM module. This illumination maximizes the use of the condenser by programming the illumination in the ring shape instead of using the physical annulus. Therefore, the ring can be generated to fill the NA of the condenser, allowing for the maximum NA possible. Fig. 1b shows an illustration comparing the regular phase contrast illumination versus the programmed ring illumination. It can be clearly seen that the programmed illumination generates a higher angle, resulting in higher resolution. Therefore, this system can achieve the transverse resolution up to 200 nm for white light, given that the NA of the objective and the condenser are both 1.4. Furthermore, higher NA of the condenser, equivalent to larger coverage in the spatial frequency associated with the optical axis, also improves optical sectioning and tomographic imaging capability. Since the illumination ring is not determined by the physical annulus in the condenser, it is possible to match the illumination ring and the phase ring on the spatial light modulator (SLM) perfectly, while keeping both of the rings very narrow. Making the condenser phase ring thin, increases the spatial coherence and minimizes the coupling between scattered and unscattered light, which eradicates the halo effect and improves the quantitative information [46, 47].

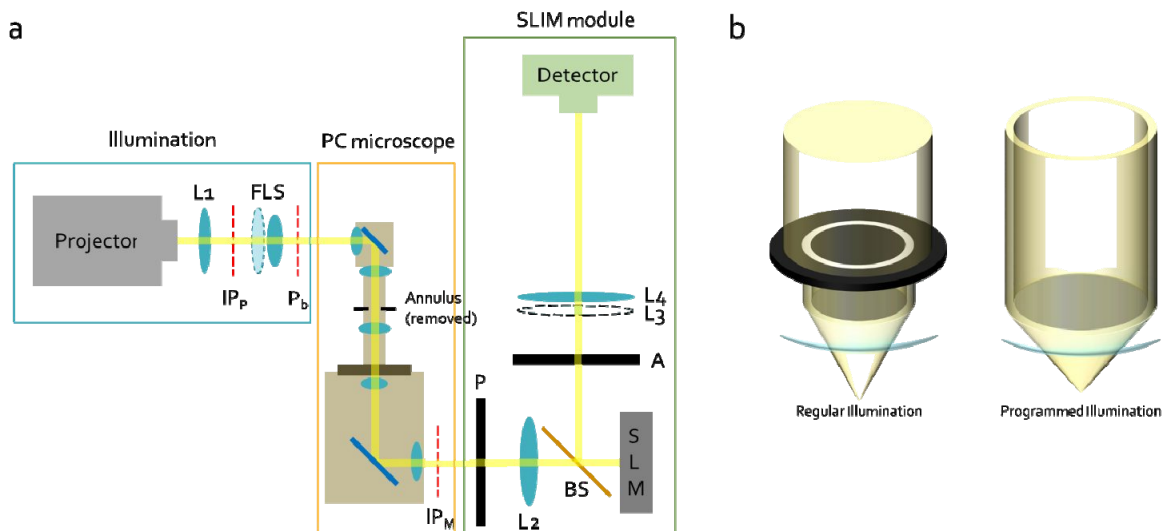


**Figure 1.** SLIM with programmable illumination. (a) Schematic of SLIM with a programmable illumination pattern. L1: Projector imaging lens,  $IP_p$ : Projector image plane, FLS: Fourier lens system,  $P_b$ : Fourier plane of the projector and the original location of halogen bulb,  $IP_M$ : Image plane of the microscope, P: Polarizer, L2: Fourier lens, BS: Beam splitter, SLM: Spatial light modulator, A: Analyzer, L3: Imaging lens for the Fourier plane, L4: Imaging lens. (b) Illustration of the difference in NA between the regular illumination and the programmed illumination.

The SLIM module first selects one linear polarization of the light for proper modulation at the SLM, and generates an image of the back focal plane of the objective at the SLM plane. On the SLM, four patterns are projected to add four different phase shift ( $0, \pi/2, \pi, \text{ or } 3\pi/2$ ) to the reference light (the original illumination pattern), and through the analyzer and the imaging lens (L4), the four interferograms are formed at the detector. Imaging lens (L3) is used for the purpose of aligning the illumination with the SLM pattern. Finally the quantitative phase of the sample is retrieved through the numerical calculation using these four frames.

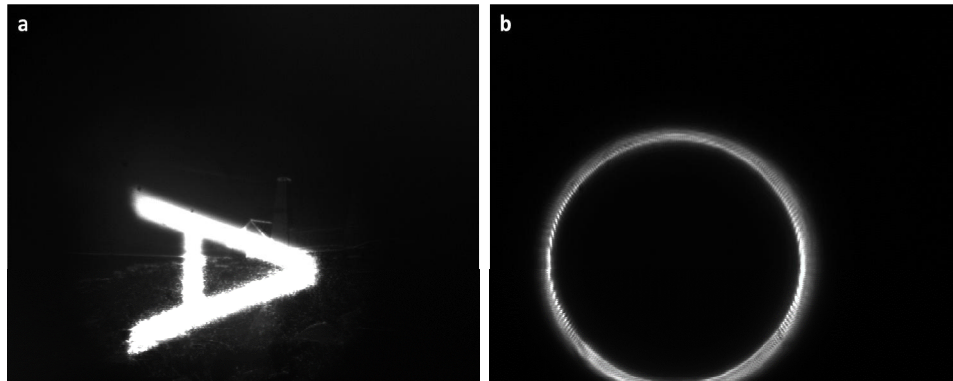


**Figure 2.** SLM plane of the setup. (a) Co-focusing the projector pattern and the SLM pattern. (b) A ring illumination projected onto the SLM plane, thus, onto the condenser aperture plane.

With a proper alignment, the illumination pattern can be projected onto the SLM, while having its Fourier transform on the sample plane as the incident field. This alignment can be ensured by imaging the SLM plane and having both the projector pattern and the SLM pattern focused simultaneously. Figure 2a shows an image of the SLM plane when such alignment is achieved. By projecting a ring pattern, this system now can perform a traditional phase contrast imaging with an optimized illumination ring.

### 3. RESULTS

In order to perform SLIM with a projector illumination, a ring pattern equivalent to 0.3 condenser NA has been created and focused on the condenser aperture plane. For a 40x/0.75NA objective, because this new ring illumination is larger than the physical ring aperture, this system is now expected to have a higher resolution. Moreover, a bright field objective needs to be used because the illumination ring does not match the objective phase ring anymore. Therefore, all of the phase shift comes from the SLM instead of having the  $\pi/2$  shift from the objective. Figure 3 shows the four phase contrast images of a red blood cell (RBC) sample with varying phase shifts.

Because of the missing attenuation on the reference beam that typically comes from the objective phase ring, the overall contrast of the phase contrast images are lower than the commercial phase contrast. Also, the ring from the projector is different from the original ring illumination, which is generated by spatially filtering a plane wave. Therefore, at the image plane, it does not create a perfectly uniform background and results in a brighter center. All these artifacts can be seen in all four frames shown in Fig. 3.

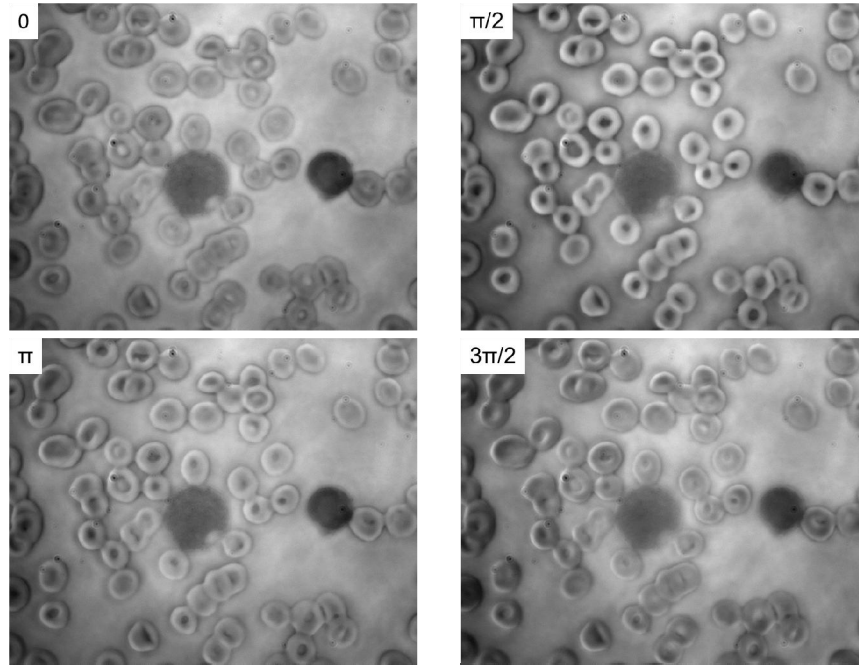


**Figure 3.** Phase contrast images of an RBC sample with varying phase shifts applied on the ring.

In order to generate a quantitative phase image from these four frames, the missing attenuation correction factor needs to be adjusted numerically as it does in the regular SLIM. Theoretically, the attenuation factor needs to be simply 1. However, due to the large mismatch between the intensity of the reference and that of the scattered field, the contrast of each phase contrast image degrades, which consequently results in an incorrect phase value. Therefore, by changing the attenuation factor, we can find the optimal value that numerically corrects for the phase value. In Fig. 4, phase images obtained by combining the four frames with varying attenuation factors are presented along with the maximum phase value of the RBC as a function of the attenuation factor.

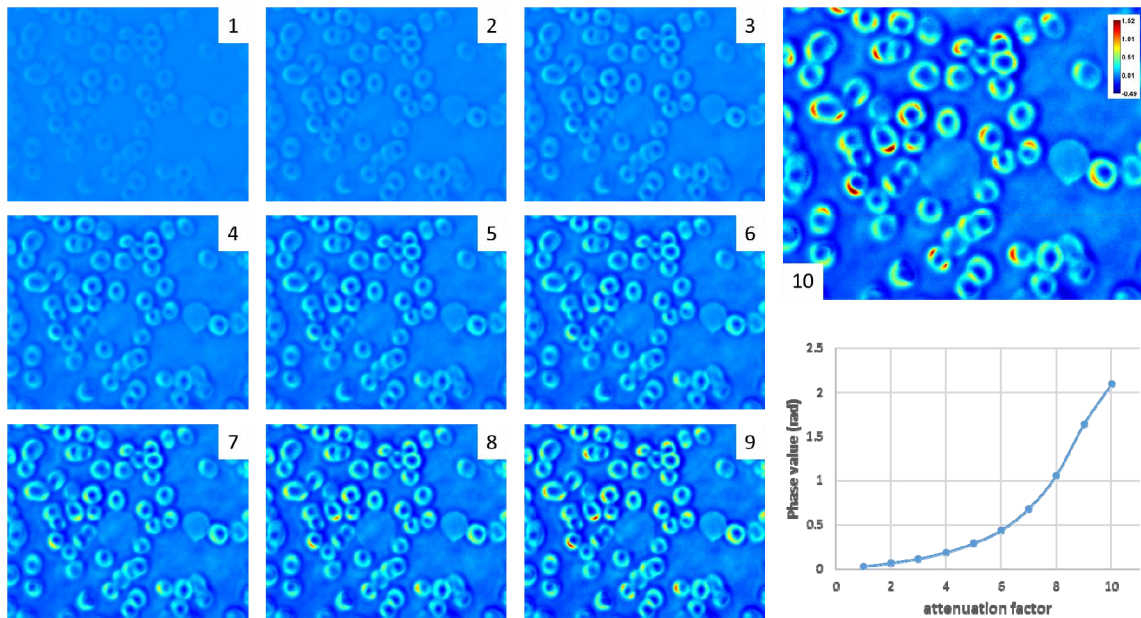


**Figure 4.** Reconstructed phase images with varying attenuation correction factors and the phase value as a function of the attenuation correction factor.

Comparing with the previously measured phase values for RBCs [34], it can be predicted that 9 as the attenuation correction factor would give the most accurate result. Using this factor, we imaged 3  $\mu\text{m}$  polystyrene beads ( $n = 1.59$ ) in immersion oil ( $n = 1.518$ ) for quantitative phase measurement. Figure 5(a) shows the four interferograms that are taken at different phase shifts given by the SLM. Figures 5(b) and 5(c) show the phase map of imaging these beads and the profile over one bead indicated with a dashed line. The average height of the beads is 3.09 nm, which is well matched to the expected value and shows that the system correctly obtains quantitative phase. Notice that the halo artifact is mostly removed, due to the perfect matching of the illumination and phase modulation rings.

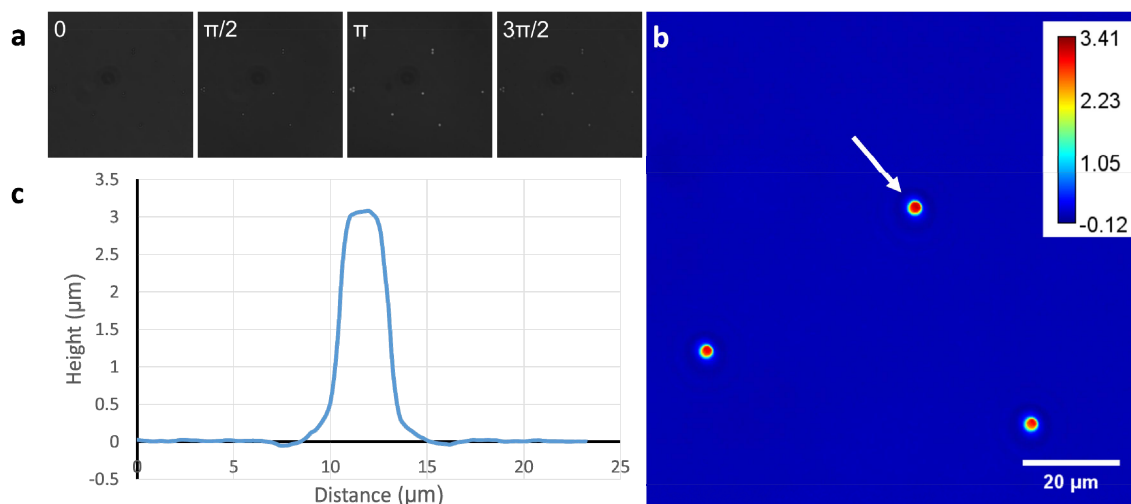


**Figure 5.** Measurement of 3  $\mu\text{m}$  beads with SLIM upgraded with programmable illumination. (a) Four interferograms with phase shift indicated on the top left of each frame. (b) Reconstructed phase map. Color bar is in  $\mu\text{m}$ . (c) Profile of the bead indicated in (b) by the arrow.

#### 4. SUMMARY

In summary, we have presented an upgraded spatial light interference microscopy system with a programmable illumination from a commercial projector. We replaced the halogen lamp with a projector, phase contrast objective with a bright field objective, and added a SLIM module for quantitative phase imaging. The resulting images show, with a proper calibration for the attenuation constant, reasonable values matching closely with the traditional methods. This upgrade allows for a better shaped ring illumination for phase contrast microscopy with a larger effective NA for the condenser. Thus, this upgraded system is expected to provide a higher resolution. Moreover, due to the improved match between the illumination and phase rings, the halo artifact appears to be removed by a large degree.

#### ACKNOWLEDGMENTS

This work was supported by the National Science Foundation CBET-1040461 MRI with matching funds from the University of Illinois (GP, LG), Agilent Laboratories (GP) and Beckman Graduate Fellowship (TK). For more information, visit <http://light.ece.illinois.edu/>

## REFERENCES

- [1] G. Popescu, [Quantitative phase imaging of cells and tissues] McGraw Hill, (2011).
- [2] T. Kim, R. Zhou, L. L. Goddard *et al.*, “Breakthroughs in Photonics 2013: Quantitative Phase Imaging: Metrology Meets Biology,” *Photonics Journal*, IEEE, 6(2), 1-9 (2014).
- [3] M. Mir, A. Bergamaschi, B. S. Katzenellenbogen *et al.*, “Highly Sensitive Quantitative Imaging for Monitoring Single Cancer Cell Growth Kinetics and Drug Response,” *PLoS ONE*, 9(2), e89000 (2014).
- [4] M. Mir, Z. Wang, Z. Shen *et al.*, “Optical measurement of cycle-dependent cell growth,” *Proceedings of the National Academy of Sciences*, 108(32), 13124-13129 (2011).
- [5] M. Mir, T. Kim, A. Majumder *et al.*, “Label-Free Characterization of Emerging Human Neuronal Networks,” *Sci. Rep.*, 4, (2014).
- [6] B. Bhaduri, D. Wickland, R. Wang *et al.*, “Cardiomyocyte Imaging Using Real-Time Spatial Light Interference Microscopy (SLIM),” *Plos One*, 8(2), (2013).
- [7] H. V. Pham, C. Edwards, L. L. Goddard *et al.*, “Fast phase reconstruction in white light diffraction phase microscopy,” *Applied Optics*, 52(1), A97-A101 (2013).
- [8] Y. Park, C. A. Best-Popescu, R. R. Dasari *et al.*, “Light scattering of human red blood cells during metabolic remodeling of the membrane,” *Journal of Biomedical Optics*, 16(1), 011013 (2011).
- [9] H. F. Ding, E. Berl, Z. Wang *et al.*, “Fourier Transform Light Scattering of Biological Structure and Dynamics,” *Ieee Journal of Selected Topics in Quantum Electronics*, 16(4), 909-918 (2010).
- [10] Y. K. Park, M. Diez-Silva, G. Popescu *et al.*, “Refractive index maps and membrane dynamics of human red blood cells parasitized by *Plasmodium falciparum*,” *Proceedings of the National Academy of Sciences*, 105(37), 13730-13735 (2008).
- [11] G. Popescu, Y. Park, N. Lue *et al.*, “Optical imaging of cell mass and growth dynamics,” *The American Journal of Physiology - Cell Physiology*, 295(2), C538-44 (2008).
- [12] G. Popescu, Y. Park, W. Choi *et al.*, “Imaging red blood cell dynamics by quantitative phase microscopy,” *Blood Cells Molecules and Diseases*, 41(1), 10-16 (2008).
- [13] G. Popescu, [Quantitative Phase Imaging of Nanoscale Cell Structure and Dynamics] Academic Press, San Diego, Chapter 5 (2008).
- [14] G. Popescu, T. Ikeda, R. R. Dasari *et al.*, “Diffraction phase microscopy for quantifying cell structure and dynamics,” *Optics Letters*, 31(6), 775-777 (2006).
- [15] T. Kim, S. Sridharan, and G. Popescu, “Gradient field microscopy of unstained specimens,” *Opt. Express*, 20(6), 6737-6745 (2012).
- [16] T. Kim, and G. Popescu, “Laplace field microscopy for label-free imaging of dynamic biological structures,” *Optics Letters*, 36(23), 4704-4706 (2011).
- [17] V. Crecea, B. W. Graf, T. Kim *et al.*, “High Resolution Phase-Sensitive Magnetomotive Optical Coherence Microscopy for Tracking Magnetic Microbeads and Cellular Mechanics,” *Selected Topics in Quantum Electronics*, IEEE Journal of, PP(99), 1-1 (2013).
- [18] N. T. Shaked, M. T. Rinehart, and A. Wax, “Dual-interference-channel quantitative-phase microscopy of live cell dynamics,” *Optics Letters*, 34(6), 767-769 (2009).
- [19] N. Pavillon, J. Kühn, C. Moratal *et al.*, “Early Cell Death Detection with Digital Holographic Microscopy,” *PLoS ONE*, 7(1), e30912 (2012).
- [20] R. Wang, Z. Wang, L. Millet *et al.*, “Dispersion-relation phase spectroscopy of intracellular transport,” *Optics Express*, 19(21), 20571-20579 (2011).
- [21] Z. Wang, L. Millet, V. Chan *et al.*, “Label-free intracellular transport measured by spatial light interference microscopy,” *Journal of Biomedical Optics*, 16, 026019 (2011).
- [22] N. Lue, W. Choi, G. Popescu *et al.*, “Synthetic aperture tomographic phase microscopy for 3D imaging of live cells in translational motion,” *Optics express*, 16(20), 16240-16246 (2008).

- [23] Z. Wang, D. L. Marks, P. S. Carney *et al.*, “Spatial light interference tomography (SLIT),” *Optics Express*, 19(21), 19907-19918 (2011).
- [24] M. Mir, S. D. Babacan, M. Bednarz *et al.*, “Visualizing Escherichia coli sub-cellular structure using sparse deconvolution Spatial Light Interference Tomography,” *PLoS One*, 7(6), e39816 (2012).
- [25] T. Kim, R. Zhou, M. Mir *et al.*, “White-light diffraction tomography of unlabelled live cells,” *Nat Photon*, 8(3), 256-263 (2014).
- [26] K. Kim, Z. Yaqoob, K. Lee *et al.*, “Diffraction optical tomography using a quantitative phase imaging unit,” *Optics Letters*, 39(24), 6935-6938 (2014).
- [27] Y. Kim, H. Shim, K. Kim *et al.*, “Profiling individual human red blood cells using common-path diffraction optical tomography,” *Sci. Rep.*, 4, (2014).
- [28] Y. Kim, H. Shim, K. Kim *et al.*, “Common-path diffraction optical tomography for investigation of three-dimensional structures and dynamics of biological cells,” *Optics Express*, 22(9), 10398-10407 (2014).
- [29] K. Kim, K. S. Kim, H. Park *et al.*, “Real-time visualization of 3-D dynamic microscopic objects using optical diffraction tomography,” *Optics Express*, 21(26), 32269-32278 (2013).
- [30] Y. Cotte, F. Toy, P. Jourdain *et al.*, “Marker-free phase nanoscopy,” *Nat Photon*, 7(2), 113-117 (2013).
- [31] W. Choi, C. Fang-Yen, K. Badizadegan *et al.*, “Tomographic phase microscopy,” *Nat Meth*, 4(9), 717-719 (2007).
- [32] B. Bhaduri, M. Kandel, C. Brugnara *et al.*, “Optical Assay of Erythrocyte Function in Banked Blood,” *Sci. Rep.*, 4, (2014).
- [33] H. Pham, B. Bhaduri, K. Tangella *et al.*, “Real time blood testing using quantitative phase imaging,” *PLoS ONE*, 8(2), e55676 (2013).
- [34] M. Mir, K. Tangella, and G. Popescu, “Blood testing at the single cell level using quantitative phase and amplitude microscopy,” *Biomedical Optics Express*, 2(12), 3259-3266 (2011).
- [35] Y. K. Park, M. Diez-Silva, D. Fu *et al.*, “Static and dynamic light scattering of healthy and malaria-parasite invaded red blood cells,” *Journal of biomedical optics*, 15, 020506 (2010).
- [36] M. Mir, Z. Wang, K. Tangella *et al.*, “Diffraction Phase Cytometry: blood on a CD-ROM,” *Opt. Express*, 17(4), 2579-2585 (2009).
- [37] M. Hunter, V. Backman, G. Popescu *et al.*, “Tissue self-affinity and polarized light scattering in the born approximation: a new model for precancer detection,” *Physical review letters*, 97(13), 138102 (2006).
- [38] Z. Wang, G. Popescu, K. V. Tangella *et al.*, “Tissue refractive index as marker of disease (Journal Paper),” *Journal of Biomedical Optics*, 16(11), 116017 (2011).
- [39] T. Kim, S. Sridharan, A. Kajdacsy-Balla *et al.*, “Gradient field microscopy for label-free diagnosis of human biopsies,” *Appl. Opt.*, 52(1), A92-A96 (2013).
- [40] C. Edwards, A. Arbabi, G. Popescu *et al.*, “Optically monitoring and controlling nanoscale topography during semiconductor etching,” *Light Sci Appl*, 1, e30 (2012).
- [41] C. Edwards, K. Wang, R. Zhou *et al.*, “Digital projection photochemical etching defines gray-scale features,” *Opt. Express*, 21(11), 13547-13554 (2013).
- [42] S.-W. Hwang, G. Park, C. Edwards *et al.*, “Dissolution Chemistry and Biocompatibility of Single-Crystalline Silicon Nanomembranes and Associated Materials for Transient Electronics,” *ACS Nano*, (2014).
- [43] C. Edwards, R. Zhou, S.-W. Hwang *et al.*, “Diffraction phase microscopy: monitoring nanoscale dynamics in materials science [Invited],” *Applied Optics*, 53(27), G33-G43 (2014).
- [44] C. Edwards, S. J. McKeown, J. Zhou *et al.*, “In situ measurements of the axial expansion of palladium microdisks during hydrogen exposure using diffraction phase microscopy,” *Optical Materials Express*, 4(12), 2559-2564 (2014).

- [45] Z. Wang, L. J. Millet, M. Mir *et al.*, “Spatial light interference microscopy (SLIM),” *Optics Express*, 19(2), 1016-1026 (2011).
- [46] C. Edwards, B. Bhaduri, T. Nguyen *et al.*, “Effects of spatial coherence in diffraction phase microscopy,” *Optics Express*, 22(5), 5133-5146 (2014).
- [47] T. H. Nguyen, C. Edwards, L. L. Goddard *et al.*, “Quantitative phase imaging with partially coherent illumination,” *Optics Letters*, 39(19), 5511-5514 (2014).